J Mol Model (2009) 15:1193–1201
DOI 10.1007/s00894-009-0479-0

ORIGINAL PAPER

# Methyl 2-methoxy-7-(4-methylbenzoyl)-4-oxo-6-*p*-tolyl-4H-furo[3,2-*c*]pyran-3-carboxylate:A combined experimental and theoretical investigation

**Namık Özdemir · Muharrem Dinçer · İrfan Koca · İsmail Yıldırım · Orhan Büyükgüngör**

Received: 8 December 2008 / Accepted: 28 January 2009 / Published online: 5 March 2009


**Abstract** The title compound, methyl 2-methoxy-7-(4-methylbenzoyl)-4-oxo-6-*p*-tolyl-4H-furo[3,2-*c*]pyran-3-carboxylate ($C_{25}H_{20}O_7$), was prepared and characterized by IR and single-crystal X-ray diffraction (XRD). The compound crystallizes in the triclinic space group $P\,{-}1$ with $a$=8.9554 (9) Å, $b$=10.0018(10) Å, $c$=12.7454(13) Å, $\alpha$=67.678(7)°, $\beta$=89.359(8)° and $\gamma$=88.961(8)°. In addition to the molecular geometry from X-ray experiment, the molecular geometry and vibrational frequencies of the title compound in the ground state have been calculated using semiempirical AM1 and PM3 methods, as well as Hartree-Fock (HF) and density functional (B3LYP) levels of theory with 6–31G(d) basis set. To determine conformational flexibility, molecular energy profile of the title compound was obtained by semi-empirical (AM1) calculations with respect to two selected degrees of torsional freedom, which were varied from −180° to +180° in steps of 10°. Besides, frontier molecular orbitals (FMO) analysis and thermodynamic properties of the title compound were performed by the B3LYP/6–31G(d) method.

**Keywords** Ab-initio calculation · AM1 and PM3 semi-empirical methods · B3LYP · Conformational analysis · Hartree-Fock · Vibrational assignment · X-ray structure determination

## Introduction

The title compound synthesized by a multicomponent reaction is a derivative of furo[3,2-*c*]pyran-4-one, which are reported as free radical scavengers and exhibits cytotoxic activity [1–3]. 4-Hydroxy derivative of furo[3,2-*c*]pyran compound is known as Patulin which is a potent antibiotic and is a mycotoxin produced by several species of aspergillus and penicillium mainly found in unfermented apple, grape juice and field crops [4, 5]. Some 4*H*-pyran derivatives are potential bioactive compounds, such as calcium antagonists [6] or potent apoptosis inducers [7, 8]. 4H-benzo[*b*]pyran and their derivatives have attracted strong interest due to their useful biological and pharmacological properties, such as anticoagulant, spasmolytic, diuretic, anticancer, antianaphylactin characteristics [9, 10]. The phellifuropyranone, 2-(3,4-dihydroxyphenyl)-6-(2′-(3,4-dihydroxyphenyl)-*E*-ethenyl)-furo[3,2-*c*]pyran-4-one, has antiproliferative activity against mouse melanoma cells and human lung cancer cells *in vitro* [11]. Some 2-amino-4H-pyrans can be employed as photoactive materials [12]. Furthermore, the 4H-pyran group is a constituent of the structures of a series of natural products [13, 14]. The known synthesis methods of furo[3,4-c]pyranones are through intramolecular hetero Diels-Alder reaction or tungsten-mediated [3+3] cycloaddition of tethered alkynes

**Electronic supplementary material** The online version of this article (doi:10.1007/s00894-009-0479-0) contains supplementary material, which is available to authorized users.

N. Özdemir (✉) · M. Dinçer · O. Büyükgüngör
Department of Physics, Faculty of Arts and Sciences,
Ondokuz Mayıs University,
55139 Kurupelit, Samsun, Turkey
e-mail: namiko@omu.edu.tr

İ. Koca
Department of Chemistry, Faculty of Arts and Sciences,
Bozok University,
66200 Yozgat, Turkey

İ. Yıldırım
Department of Chemistry, Faculty of Arts and Sciences,
Erciyes University,
38039 Kayseri, Turkey

with epoxides [15–19]. Although furopyrans are an essential part of many biologically important compounds, the synthesis and structural properties of furo[3,4-c]pyran compounds are very limited.

In this study, we present results of a detailed investigation of the synthesis and structural characterization of methyl 2-methoxy-7-(4-methylbenzoyl)-4-oxo-6-*p*-tolyl-4H-furo[3,2-*c*]pyran-3-carboxylate using single crystal X-ray, IR and quantum chemical methods, besides elemental analysis. The title compound is a novel compound synthesized firstly in our laboratories by us. To the best of our knowledge, the multicomponent reaction of dialkyl acetylene dicarboxylates with the furan-2,3-dione and triphenyl phosphine have not been previously studied and the product (title compound) is completely original.

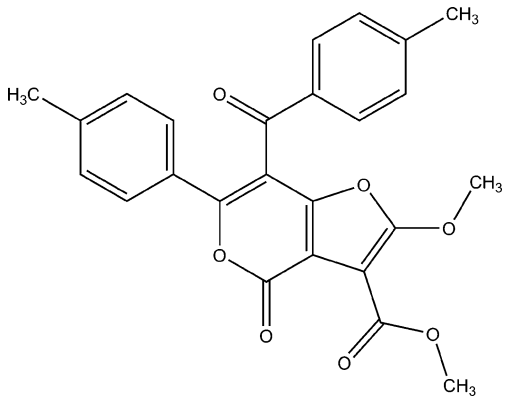


**Fig. 1** Chemical structure of the title compound

Full crystallographic data are available as supplementary material.

## Experimental

### Synthesis

Melting points were measured on an Electrothermal 9100 apparatus and are uncorrected. Elemental analysis for C and H was performed using a Leco-932 CHNS-O Elemental Analyzer. IR spectra of the compound were recorded in the range of 4000–400 $cm^{-1}$ region with a Jasco FT-IR-460 Plus spectrometer. Solvents were dried by refluxing with the appropriate drying agents and distilled before use. All other reagents were purchased from Merck, Fluka, Aldrich and used without further purification. The starting material was prepared in a manner similar to that described by Ziegler and co-workers [20] and by Yıldırım and co-workers [21, 22]. To a stirred solution of 4-(4-methylbenzoyl)-5-(4-methylphenyl)furan-2,3-dione (1 mmol) and dialkyl acetylene dicarboxylates (1 mmol) in benzene (20 ml) was added dropwise triphenyl phosphine (1 mmol) in benzene (5 ml), and the mixture was stirred at ambient temperature for 10 min. Then, the mixture was refluxed in boiling benzene for 15 min. The solvent was removed under reduced pressure, and the residue was triturated with methanol to give yellow crystals which were filtered off and recrystallized from methanol (Fig. 1) (yield: 0.22 g, 51%; m.p. 441–443 K). IR (KBr, ν, $cm^{-1}$): 1766, 1714, 1655 (C=O), 1604–1475 (C=C), 1230 (C–O). Analysis calculated for $C_{25}H_{20}O_7$ (432.42 g $mol^{-1}$): C 69.44, H 4.66%; found: C 69.56, H 4.79%.

#### *Crystal data for the title compound*

CCDC 701463, $C_{25}H_{20}O_7$, $M_w$=432.41, triclinic, space group $P$ −1; $Z$=2, $a$=8.9554(9), $b$=10.0018(10), $c$=12.7454(13) Å, $\alpha$=67.678(7), $\beta$=89.359(8), $\gamma$=88.961(8)°; $V$=1055.87(18) $Å^3$, $F(000)$=452, $D_x$=1.360 g $cm^{-3}$.

### Computational details

Theoretical calculations were carried out using semi-empirical AM1, PM3 and *ab initio* HF/6–31G(d) and density functional B3LYP/6–31G(d) [23–25] quantum mechanical methods. For modeling, the initial guess of the title compound was first obtained from the X-ray coordinates. Molecular geometry is restricted and all the calculations are performed without specifying any symmetry for the title molecule by using Gaussian 03 Program package [26] on a personal computer. Then vibrational frequencies for optimized molecular structures have been calculated. The vibrational frequencies for these species are scaled by 0.9532, 0.9761, 0.8929 and 0.9613 [27], respectively. To identify low energy conformations, two selected degrees of torsional freedom, $T$(C2–C1–C8–C9) and $T$(C2–C15–C16–C17), were varied from −180° to +180° in steps of 10°, and the molecular energy profiles were obtained at the semi-empirical AM1 level.

## Results and discussion

### IR spectroscopy

The vibrational bands assignments have been made by using Gauss-View molecular visualization program [28]. Frequency calculations at the same levels of theory revealed no imaginary frequencies, indicating that an optimal geometry at these levels of approximation was found for the title compound.

We have compared our calculation of the title compound with their experimental results. The experimental C=O stretching modes were observed at 1766, 1714 and 1655 $cm^{-1}$, that have been calculated with AM1, PM3, HF and B3LYP at 2017–1952–1940, 1982–1923–1918,

1816–1761–1757 and 1790–1709–1676 $cm^{-1}$, respectively. The two bands at 1604 and 1475 $cm^{-1}$, which can be attributed to the C=C stretching vibrations, have been calculated at 1806–1728 $cm^{-1}$ for AM1, 1801–1772 $cm^{-1}$ for PM3, 1639–1593 $cm^{-1}$ for HF and 1581–1519 $cm^{-1}$ for B3LYP. Finally, the experimental C–O stretching mode appeared at 1230 $cm^{-1}$ has been calculated at 1234, 1215, 1288 and 1246 $cm^{-1}$ for AM1, PM3, HF and B3LYP, respectively. It is seen from these values that the results of B3LYP method has shown a better fit to experimental ones than the others in evaluating vibrational frequencies.

## Crystal structure

The title compound, an Ortep-3 [29] view of which is shown in Fig. 2, crystallizes in the triclinic space group *P*−1 with two molecules in the unit cell. The core of the molecule consists of *trans*-fused [30] pyran (*A*) and furan (*B*) rings. The C3=C6 double bond at the *AB* ring junction is 1.3541(17) Å and compares well with the value reported previously [1.357(3) Å, 31]. The 4*H*-furo[3,2-*c*]pyran fragment is planar within experimental error. The angle between the best planes through ring *A* (atoms O1/C1/C2/C3/C6/C7) and ring *B* (atoms O2/C3/C4/C5/C6) is 1.38(9), while the crossed torsion angles at the junction, *i.e.*, O2–C3–C6–C7 and C2–C3–C6–C5 are −176.07(12) and 178.25(13)°, respectively.

In the molecule, the pyran ring adopts a flattened boat conformation, with a deviation of atoms C2 and C7 from the O1/C1/C3/C6 plane [planar within −0.0376(9) Å] of 0.0469(9) and 0.0620(9) Å, respectively. The *p*-tolyl ring is rotated by 14.45(7)° with respect to the furo-pyran fragment and the C1–C8 bond distance of 1.465(2) Å denotes the absence of conjugation between the two π-delocalized systems. This orientation is stabilized by a short intramolecular contact between the carboxyl O and H9 atoms

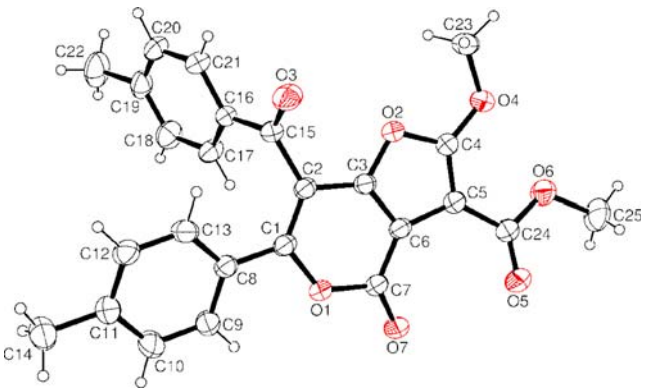


**Fig. 2** Perspective view of the title compound showing the atom-numbering scheme. Displacement ellipsoids are drawn at the 30% probability level and H atoms are shown as small spheres of arbitrary radii

**Table 1** Hydrogen bonding geometry (Å, °) for the title compound

| D—H•••A | D—H | H•••A | D•••A | D—H•••A |
|---|---|---|---|---|
| C9—H9A•••O1 | 0.93 | 2.36 | 2.6940(18) | 101 |
| C23—H23A•••O7$^{i}$ | 0.96 | 2.60 | 3.5488(19) | 171 |
| C23—H23B•••O3$^{ii}$ | 0.96 | 2.49 | 3.388(2) | 156 |

Symmetry codes: (i) *x*, *y*+1, *z*; (ii) 1 − *x*, 2 − *y*, 1 − *z*

[C9•••O1=2.6940(18) Å and C9–H9•••O1=101°] forming an *S*(5) motif [32]. However, the methylbenzoyl ring plane is inclined at an angle of 64.36(3)° to the furo-pyran ring plane.

The bond distances and angles of the 4*H*-furo[3,2-*c*] pyran moiety are in good agreement with the corresponding values reported for such fragments in the Cambridge Structural Database (CSD, Version 5.28) [33], which has been searched using *ConQuest* software (Version 3.6) [34]. The furan ring bond distances indicate π-electron delocalization existing over the whole twocyclic system. An important asymmetry in the O–C–O and O–C–C bond angles has been detected [O7–C7–O1=116.21(12)° and O7–C7–C6=130.43(13)°], which was also seen in other similar compounds reported in the CSD.

The geometry of the carboxylate group is normal and slightly rotated out of the plane of the furan ring with a dihedral angle of 16.58(13)°. In the carboxylate group, the C24—O6 bond [1.3321(18) Å] is longer than the C24–O5 bond [1.1993(18) Å] and considerably shorter than C25–O6 [1.447(2) Å], which demonstrates the conjugation of atom O6 with C24–O5.

Inspection of the displacement ellipsoids of the (C16–C21) phenyl ring show a large anisotropy of the C18, C19, C20 and C21 atoms and a somewhat large dispersion of the ring C–C bond lengths [1.367(2) – 1.3918(19) Å]. This suggests that a minor disorder of the ring, of either static or dynamic nature, may be present, which is not unexpected due to the probable low potential barrier for rotation around the single C15–C16 bond.

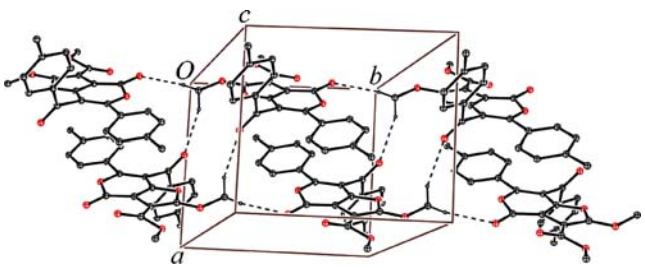


**Fig. 3** Part of the crystal structure of the title compound, showing the formation of a [010] chain of alternating $R_2^2(18)$ and $R_4^4(20)$ rings. For the sake of clarity, H atoms not involved in the motifs shown have been omitted

**Table 2** Optimized and experimental geometries of the title compound in the ground state

| Parameters | X-ray | AM1 | PM3 | HF/6–31G(d) | B3LYP/6–31G(d) |
|---|---|---|---|---|---|
| Bond lengths (Å) | | | | | |
| O1–C1 | 1.3726(15) | 1.3738 | 1.3691 | 1.3473 | 1.3612 |
| O1–C7 | 1.4018(17) | 1.4113 | 1.3931 | 1.3734 | 1.4235 |
| O2–C3 | 1.3679(15) | 1.3948 | 1.3833 | 1.3370 | 1.3612 |
| O2–C4 | 1.3627(16) | 1.4023 | 1.3817 | 1.3424 | 1.3662 |
| O3–C15 | 1.2134(17) | 1.2369 | 1.2153 | 1.1946 | 1.2234 |
| O4–C4 | 1.3124(16) | 1.3427 | 1.3440 | 1.3036 | 1.3205 |
| O4–C23 | 1.4455(17) | 1.4388 | 1.4147 | 1.4221 | 1.4397 |
| O5–C24 | 1.1993(18) | 1.2391 | 1.2171 | 1.1945 | 1.2207 |
| O6–C24 | 1.3321(18) | 1.3656 | 1.3645 | 1.3130 | 1.3424 |
| O6–C25 | 1.447(2) | 1.4297 | 1.4121 | 1.4158 | 1.4349 |
| O7–C7 | 1.1998(15) | 1.2247 | 1.2080 | 1.1805 | 1.2040 |
| C1–C2 | 1.3551(19) | 1.3752 | 1.3688 | 1.3419 | 1.3727 |
| C1–C8 | 1.465(2) | 1.4647 | 1.4751 | 1.4788 | 1.4721 |
| C2–C3 | 1.4157(18) | 1.4230 | 1.4314 | 1.4335 | 1.4215 |
| C2–C15 | 1.5041(17) | 1.4844 | 1.4962 | 1.5120 | 1.5134 |
| C3–C6 | 1.3541(17) | 1.3970 | 1.3895 | 1.3460 | 1.3771 |
| C4–C5 | 1.3613(18) | 1.3949 | 1.3854 | 1.3563 | 1.3814 |
| C5–C6 | 1.4443(19) | 1.4514 | 1.4449 | 1.4596 | 1.4544 |
| C5–C24 | 1.4603(19) | 1.4462 | 1.4701 | 1.4735 | 1.4740 |
| C6–C7 | 1.4280(19) | 1.4371 | 1.4501 | 1.4504 | 1.4451 |
| C15–C16 | 1.473(2) | 1.4756 | 1.4892 | 1.4907 | 1.4899 |
| RMSE[a] | | 0.024 | 0.020 | 0.019 | 0.014 |
| Max. difference[a] | | 0.043 | 0.035 | 0.031 | 0.023 |
| Bond angles (°) | | | | | |
| O1–C7–O7 | 116.21(12) | 109.7888 | 108.2148 | 117.5054 | 116.4774 |
| O2–C4–O4 | 116.61(11) | 106.1645 | 104.5542 | 111.4288 | 110.9841 |
| O5–C24–O6 | 123.44(13) | 117.8300 | 119.8795 | 123.6524 | 123.4448 |
| O1–C1–C2 | 119.98(12) | 122.8865 | 123.9722 | 120.8828 | 120.7112 |
| O1–C7–C6 | 113.37(11) | 116.3521 | 117.8626 | 112.7127 | 112.4188 |
| O1–C1–C8 | 111.47(11) | 110.8733 | 111.0955 | 111.6806 | 111.9304 |
| O2–C3–C2 | 122.13(11) | 125.4334 | 126.3830 | 123.2757 | 123.2017 |
| O2–C4–C5 | 112.32(12) | 112.0594 | 112.8736 | 111.1441 | 111.3107 |
| O2–C3–C6 | 110.68(11) | 110.8621 | 110.8207 | 110.6591 | 110.3659 |
| O3–C15–C2 | 118.75(13) | 120.8585 | 120.4917 | 118.7618 | 118.6871 |
| O3–C15–C16 | 121.79(12) | 122.1333 | 122.6997 | 121.6106 | 121.6960 |
| O4–C4–C5 | 131.07(13) | 141.7518 | 142.5090 | 137.4106 | 137.6781 |
| O5–C24–C5 | 125.21(14) | 127.9046 | 127.0719 | 124.3631 | 125.0683 |
| O6–C24–C5 | 111.32(12) | 114.2636 | 113.0320 | 111.9813 | 111.4869 |
| O7–C7–C6 | 130.43(13) | 133.8591 | 133.9204 | 129.7780 | 131.0986 |
| C1–O1–C7 | 126.35(10) | 122.5955 | 121.1472 | 127.9064 | 127.1569 |
| C1–C2–C3 | 114.27(11) | 115.5396 | 115.8237 | 113.9986 | 114.2959 |
| C1–C2–C15 | 128.37(12) | 124.6164 | 123.5462 | 126.6135 | 126.3524 |
| C2–C1–C8 | 128.55(12) | 126.2257 | 124.9323 | 127.4356 | 127.3505 |
| C2–C3–C6 | 127.16(12) | 123.7039 | 122.7958 | 126.0419 | 126.3955 |
| C2–C15–C16 | 119.30(11) | 116.9995 | 116.8082 | 119.5769 | 119.5449 |
| C3–O2–C4 | 105.70(9) | 105.0859 | 104.9945 | 107.8692 | 107.1584 |
| C3–C2–C15 | 117.36(11) | 119.8333 | 120.6079 | 119.3523 | 119.2956 |
| C3–C6–C5 | 107.03(11) | 107.0129 | 107.0164 | 106.0200 | 106.5537 |

**Table 2** (continued)

| Parameters | X-ray | AM1 | PM3 | HF/6–31G(d) | B3LYP/6–31G(d) |
|---|---|---|---|---|---|
| C3–C6–C7 | 117.95(12) | 118.8682 | 118.3788 | 118.2919 | 118.8823 |
| C4–O4–C23 | 117.98(11) | 116.6950 | 116.9971 | 122.1704 | 120.3296 |
| C4–C5–C6 | 104.26(11) | 104.9773 | 104.2870 | 104.2844 | 104.5835 |
| C4–C5–C24 | 126.36(13) | 127.4893 | 128.7839 | 126.5244 | 126.3585 |
| C5–C6–C7 | 134.90(12) | 134.1129 | 134.5886 | 135.4924 | 134.4082 |
| C6–C5–C24 | 129.04(12) | 127.5332 | 126.9209 | 129.1517 | 128.9421 |
| C24–O6–C25 | 115.85(13) | 116.42714 | 118.4699 | 117.6338 | 115.8829 |
| RMSE[a] | | 3.7 | 4.2 | 1.9 | 1.8 |
| Max. difference[a] | | 10.7 | 12.1 | 6.3 | 6.6 |
| Torsion angles (°) | | | | | |
| O1–C7–C6–C5 | 175.90(14) | 179.0384 | 179.4460 | 177.9968 | 177.6492 |
| O1–C1–C8–C13 | 162.68(13) | 138.2606 | 114.0606 | 141.9995 | 146.6464 |
| O2–C3–C6–C7 | –176.07(12) | 179.0386 | 178.3952 | 177.1575 | 177.7317 |
| O2–C4–O4–C23 | 9.87(19) | 174.0149 | 172.3945 | −150.8921 | −154.7335 |
| O5–C24–C5–C4 | 160.07(16) | 14.3593 | 51.5179 | 26.6085 | 27.4874 |
| O6–C24–C5–C6 | 169.79(14) | 15.0316 | 54.2235 | 29.9005 | 32.0433 |
| C2–C3–C6–C5 | 178.25(13) | −179.9208 | 179.8785 | 179.7471 | 179.4611 |
| C2–C1–C8–C9 | 164.48(16) | 138.3580 | 114.8978 | 142.6816 | 149.5630 |
| C2–C15–C16–C17 | 2.5(2) | 3.8335 | −23.4291 | −3.8474 | −5.4092 |
| C5–C4–O4–C23 | −169.99(15) | −8.0706 | −10.9733 | 27.4372 | 23.1195 |
| C5–C24–O6–C25 | 176.37(15) | −177.7555 | −174.6525 | −174.1826 | −174.1550 |

[a] RMSE and maximum differences between the bond lengths and the bond angles computed by the theoretical method and those obtained from X-ray diffraction

The crystal structure is stabilized by two C–H•••$O_{carbonyl}$, in which the methyl group acts as double donors (Table 1), and two π−π stacking (face-to-face) interactions. In the title compound, methyl atom C23 in the molecule at (*x*, *y*, *z*) acts as hydrogen-bond donor, *via* atoms H23A and H23B, respectively, to carbonyl atoms O7 at (*x*, *y*+1, *z*) and O3 at (1 − *x*, 2 − *y*, 1 − *z*). Propagation by inversion and translation of these two interactions generates a chain of edge-fused rings running parallel to the [010] direction, with $R_2^2(18)$ [32] and $R_4^4(20)$ rings (Fig. 3). The $R_4^4(20)$ motif is reinforced by two aromatic π—π stacking interactions. The *p*-tolyl rings and the 4*H*-furo[3,2-*c*]pyran moieties in the molecules at (*x*, *y*, *z*) and (1 − *x*, 1 − *y*, 1 − *z*) are mutually parallel, with an interplanar spacing of 3.5734 (7) Å between the *p*-tolyl and furan rings, and with an interplanar spacing of 3.5170(5) Å between the *p*-tolyl and pyran rings, the corresponding ring-centroid separations being 3.7816(10) and 3.7350(9) Å, respectively.

## Theoretical structures

Some selected geometric parameters experimentally obtained and theoretically calculated by AM1, PM3, HF/6–31G(d) and B3LYP/6–31G(d) are listed in Table 2. When the X-ray structure of the title compound is compared with its optimized counterparts (see Fig. 4), conformational discrepancies are observed between them. The most remarkable discrepancies exist in the orientation of the methoxy and carboxylate groups of the title compound. In all of the calculated structures, these two groups are oriented toward one another, while these are oriented in opposite sides at the solid state of the title compound. This orientation observed in the calculated structures allows forming an intramolecular hydrogen bond between the methyl C and carbonyl O atoms, namely C23 and O5. When the geometry of this intramolecular interaction in the optimized structures is examined, it is seen that the interaction closes to linearity from AM1 to B3LYP. The calculated H•••A, D•••A and D—H•••A values are 2.36 Å, 2.77 Å, 98.99° for AM1, 2.69 Å, 3.19 Å, 107.36° for PM3, 2.34 Å, 2.95 Å, 114.05° for HF and 2.21 Å, 2.95 Å, 122.97° for DFT, respectively.

Using the root mean square error (RMSE) for evaluation, B3LYP/6–31G(d) is the density functional theory calculation that best predicts the bond distances, with a value of 0.014 Å. The PM3 method is very close to the HF/6–31G (d) method, 0.020 and 0.019 Å, respectively, whereas the AM1 level is further off with a RMSE of 0.024 Å.

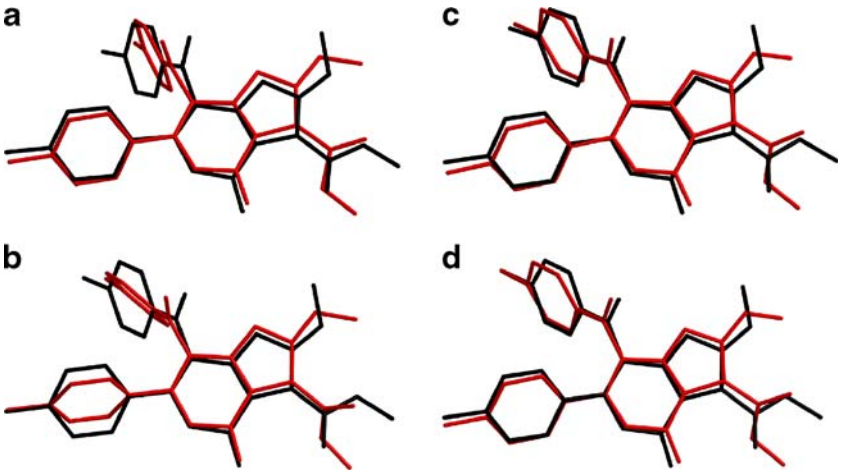


**Fig. 4** Atom-by-atom superimposition of the structures calculated (red) [**a**=AM1; **b**=PM3; **c**=HF/6–31G(d); **d**=B3LYP/6–31G(d)] over the X-ray structure (black) for the title compound. Hydrogen atoms omitted for clarity

The B3LYP calculation is again those that provide the lowest RMSE for bond angles (1.8°). The geometry obtained at the HF/6–31G(d) level coincides more with the crystalline structure than any of the semiempirical methods, as the RMSE is 1.9° compared to a value of 3.7° and 4.2° for the AM1 and PM3, respectively.

A logical method for globally comparing the structures obtained with the theoretical calculations is by superimposing the molecular skeleton with that obtained from X-ray diffraction, giving an RMSE of 0.905 Å for AM1, 0.895 Å for PM3, 0.787 Å for HF/6–31G(d), and 0.783 Å for B3LYP/6–31G(d) calculations (Fig. 4).

As can be seen in Table 2 and Fig. 4, agreement between the calculated structures and the experimentally determined X-ray crystal structure is satisfactory. The observed discrepancies between the theoretical and experimental structures most probably originate from the solid state interactions in the crystal structure. To explore the accuracy of this premise, we constructed a hydrogen-bonded initial model with four molecules residing at ($x$, $y$, $z$), ($x$, $y$+1, $z$), (1 − $x$, 2 − $y$, 1 − $z$) and (1 − $x$, 1 − $y$, 1 − $z$) using the x-ray coordinates. Then, the initial model was optimized by HF and B3LYP methods with 6–31G(d) basis set. A vibrational analysis was also carried out to check the nature of the optimized points on the potential energy surface. The vibrational frequencies calculated at the same levels of theory with the same basis set showed no imaginary frequencies approving the stable nature of the optimized structures. When the two optimized structures are examined, it is seen that the methods used in the calculations have no significant effect on the results. In other words, the computational results are close to each other. The optimized structures are shown in Fig. 5 and the mean hydrogen bonding parameters are tabulated in Table 3. As can be easily seen in Fig. 5, the first prominent feature of the optimum model is the disappearing of the different orientation of the methoxy and carboxylate groups. These two groups are oriented in opposite sides as similar to that in solid state structure and this observation clearly supports our premise. However, a more detailed investigation points out another difference existing between the optimized and X-ray crystal structures. Although the *p*-tolyl rings are almost parallel to furan-pyran rings in symmetry-related positions (interplanar dihedral being ca 14°), this arrangement is not observed in the optimized structures (interplanar dihedral being ca 45° for HF and 39° for DFT) due to the forming of a new intermolecular hydrogen bond between the methyl C and carbonyl O atoms, namely C14 and O5. This intermolecular hydrogen bond results in a tilting of *p*-tolyl rings, and so the two π—π stacking interactions have been destroyed. The mean geometry of this intermolecular

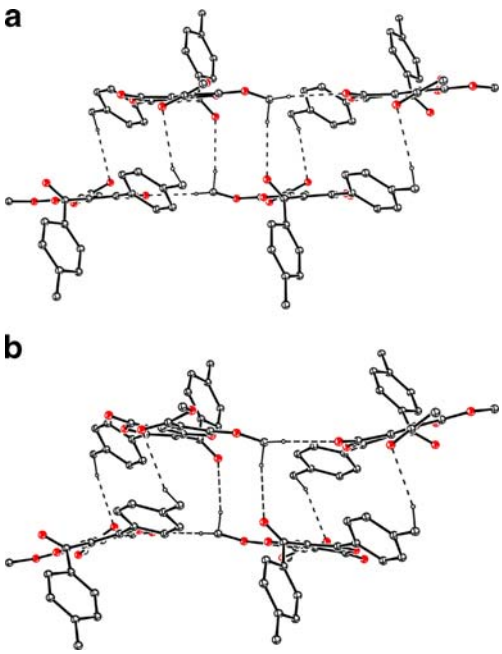


**Fig. 5** The optimized hydrogen-bonded structures of the title compound [**a**=HF/6–31G(d); **b**=B3LYP/6–31G(d)]

interaction is also given in Table 3. Finally, it is also seen from Table 3 that C23—H23B•••O3 interaction is more linear than C23—H23B•••O7 for DFT calculation as completely opposite to X-ray crystal structure.

Based on HF/6–31G(d) and B3LYP/6–31G(d) optimized geometry, the total energy of the title compound has been calculated by these two methods, which are −1482.396135 and −1491.266620 a.u., respectively. In order to define the preferential position of the two *p*-tolyl ring, namely (C8–C14) and (C16–C22) rings, with respect to 4*H*-furo[3,2-*c*] pyran moiety, a preliminary search of low energy structures was performed using AM1 computations as a function of the selected degrees of torsional freedom *T*(C2–C1–C8–C9) and *T*(C2–C15–C16–C17). The respective values of the selected degrees of torsional freedom, *T*(C2–C1–C8–C9) and *T*(C2–C15–C16–C17), are 164.48(16) and 2.5(2)° in X-ray structure, whereas the corresponding values in optimized geometries are 138.3580 and 3.8335° for AM1, 114.8978 and −23.4291° for PM3, 142.6816 and −3.8474° for HF, and 149.5630 and −5.4092° for B3LYP. Molecular energy profiles with respect to rotations about the selected torsion angles are presented in Fig. 6. According to the results, the low energy domains for *T*(C2–C1–C8–C9) are located at −40 and 140° having energy of −148.526 and −148.537 kcal $mol^{-1}$, respectively, while they are located at −170, 10 and 180° having energy of −148.541, 148.564 and 148.545 kcal $mol^{-1}$, respectively, for *T*(C2–C15–C16–C17). Energy difference between the most favorable and unfavorable conformers, which arises from rotational potential barrier calculated with respect to the two selected torsion angles, is calculated as 1.823 kcal $mol^{-1}$ for *T*(C2–C1–C8–C9) and as 1.588 kcal $mol^{-1}$ for *T*(C2–C15–C16–C17), when both selected degrees of torsional freedom are considered.

Figure 7 shows the distributions and energy levels of the HOMO − 1, HOMO, LUMO and LUMO+1 orbitals computed at the B3LYP/6–31G(d) level for the title compound. The calculations indicate that the title compound has 113 occupied molecular orbitals. Both the highest occupied molecular orbitals (HOMOs) and the lowest-lying unoccupied molecular orbitals (LUMOs) are mainly localized on the rings indicating that the HOMO-LUMO are mostly the π-antibonding type orbitals. The value of the energy separation between the HOMO and LUMO is 3.702 eV and this large energy gap indicates that the title structure is quite stable.

**Table 3** The geometric parameters of intermolecular interactions calculated by HF/6–31G(d) and B3LYP/6–31G(d)

| D—H•••A | D—H | H•••A | D•••A | D—H•••A |
|---|---|---|---|---|
| HF/6–31G(d) | | | | |
| C23—H23A•••O7 | 1.076 | 2.697 | 3.736 | 162.138 |
| C23—H23B•••O3 | 1.080 | 2.668 | 3.692 | 158.054 |
| C14—H14C•••O5 | 1.082 | 2.791 | 3.707 | 142.878 |
| B3LYP/6–31G(d) | | | | |
| C23—H23A•••O7 | 1.089 | 2.430 | 3.448 | 154.998 |
| C23—H23B•••O3 | 1.093 | 2.490 | 3.518 | 156.324 |
| C14—H14C•••O5 | 1.094 | 2.714 | 3.618 | 141.020 |

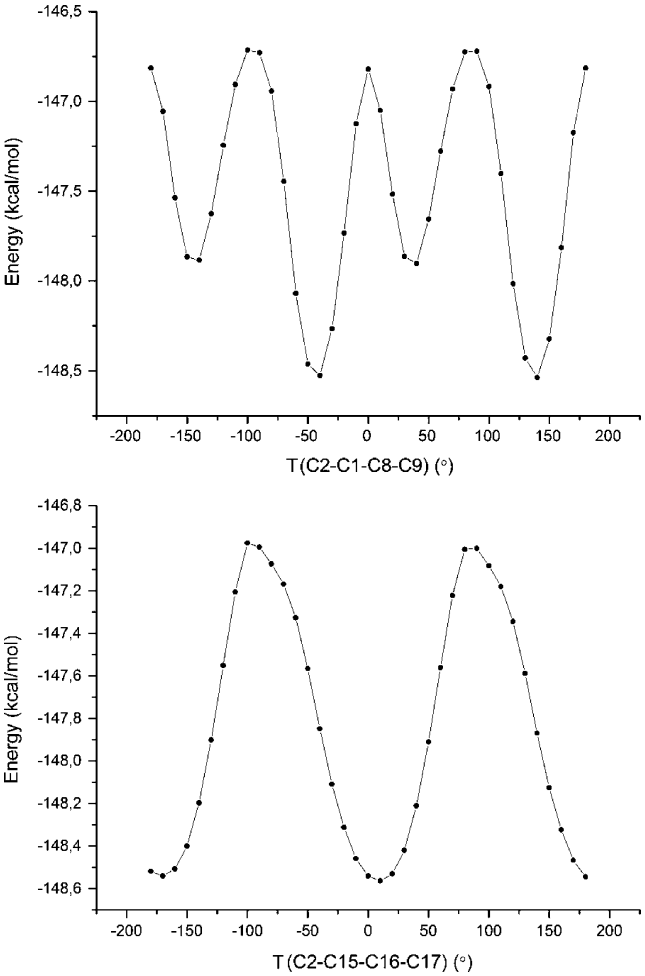


**Fig. 6** Molecular energy profiles of the optimized counterpart of the title compound against the selected degrees of torsional freedom

## Thermodynamic properties

Based on the vibrational analysis at B3LYP/6–31G(d) level and statistical thermodynamics, the standard thermodynamic functions: heat capacity ($C^{o}_{p,m}$), entropy ($S^{o}_{m}$), and enthalpy ($H^{o}_{m}$) were obtained and listed in Table 4. The scale factor for frequencies is 0.9613, which is a typical value for the B3LYP/6–31G(d) level of calculations.

As will be seen from Table 4, the standard heat capacities, entropies and enthalpies increase at any temperature from 200.0 K to 1000.0 K since increasing temperature causes an increase in the intensities of molecular vibration. For the title compound, the correlation equations

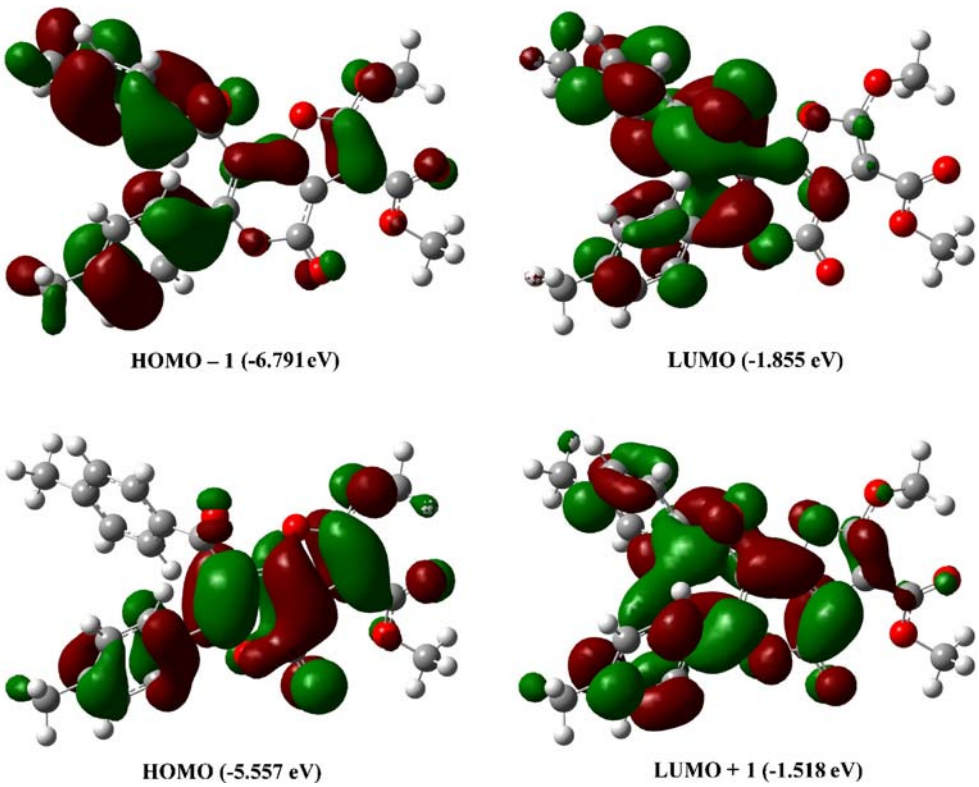


**Fig. 7** Molecular orbital surfaces and energy levels given in parentheses for the HOMO − 1, HOMO, LUMO and LUMO+1 of the title compound computed at B3LYP/6–31G(d) level

between these thermodynamic properties and temperature $T$ are as follows:

$$C^0_{p,m} = 7.81409 + 0.40406T - 1.74716 \times 10^{-4}T^2,$$
$$S^0_m = 81.39395 + 0.44592\,T - 1.06552 \times 10^{-4}T^2,$$
$$H^0_m = -13.30551 + 0.0677T + 9.5823 \times 10^{-5}T^2.$$

These equations will be helpful for the further studies of the title compound.

## Conclusions

In this study, we have synthesized by a multicomponent reaction a novel furo[3,2-*c*]pyran compound, $C_{25}H_{20}O_7$, and characterized by spectroscopic (FT-IR) and structural (XRD) techniques as well as microanalysis. As multicomponent reactions are one-pot reactions, they are easier to carry out than multistep syntheses. To fit the theoretical frequency results with experimental ones for AM1, PM3, HF and B3LYP levels, we have multiplied the data. Geometrical results from the calculations confirmed that experimental and theoretical structures have similar structural parameters. It was noted that the experimental results belong to solid phase and theoretical calculations belong to gaseous phase. In the solid state, the existence of the crystal field along with the intermolecular interactions have connected the molecules together, which result in the differences of bond parameters between the calculated and experimental values. Despite the differences observed in the geometric parameters, the general agreement is good and

**Table 4** Thermodynamic properties of the title compound at different temperatures at B3LYP/6–31G(d) level

| $T$ (K) | $C^o_{p,m}$ $(cal.mol^{-1}.K^{-1})$ | $S^o_m$ $(cal.mol^{-1}.K^{-1})$ | $H^o_m$ $(kcal.mol^{-1})$ |
|---|---|---|---|
| 200.0 | 81.52 | 165.96 | 5.28 |
| 298.1 | 112.21 | 205.02 | 14.99 |
| 300.0 | 112.79 | 205.73 | 15.20 |
| 400.0 | 142.31 | 242.87 | 28.17 |
| 500.0 | 167.44 | 277.86 | 43.91 |
| 600.0 | 187.89 | 310.62 | 61.91 |
| 700.0 | 204.44 | 341.18 | 81.75 |
| 800.0 | 217.95 | 369.66 | 103.09 |
| 900.0 | 229.11 | 396.23 | 125.66 |
| 1000.0 | 238.41 | 421.07 | 149.25 |

the theoretical calculations support the solid state structures. It is seen from the theoretical results, the results of B3LYP method have shown a better fit to experimental ones than HF in evaluating geometrical parameters and vibrational frequencies. Crystal packing of the title compound is mainly dominated by intermolecular $C_{methyl}$–H•••$O_{carbonyl}$ hydrogen bonds formed during preparation or crystallization. These hydrogen bonds supply the leading contribution to the stability and to the order of the crystal structure, and are presumably responsible for the discrepancies between the experimental and calculated structures.

**Acknowledgments** This study was supported financially by the Research Centre of Ondokuz Mayıs University (Project No: F-425).

## References

1. Mo S, Wang S, Zhou G, Yang Y, Li Y, Chen X, Shi J (2004) J Nat Prod 67:823–828
2. Kim JP, Yun B-S, Shim YK, Yoo ID (1999) Tetrahedron Lett 40:6643–6644
3. Dinçer M, Yıldırım İ, Koca İ, Özdemir N (2004) Acta Cryst E60:0207–0209
4. Florey HW, Chain E, Headley NG, Jennings M, Sanders AG, Abraham ED, Florey ME (1949) Antibiotics, 2 vols. Oxford Univ Press, London
5. Woordward RB, Singh G (1950) J Am Chem Soc 72(3):1428
6. Suarez M, Salfran E, Verdecia Y, Ochoa E, Alba L, Martin N, Martinez R, Quinteiro M, Seoane C, Novoa H, Blaton N, Peeters OM, De Ranter C (2002) Tetrahedron 58:953–960
7. Kemnitzer W, Drewe J, Jiang S, Zhang H, Wang Y, Zhao J, Jia S, Herich J, Labreque D, Storer R, Meerovitch K, Bouffard D, Rej R, Denis R, Blais C, Lamothe S, Attardo G, Gourdeau H, Tseng B, Kasibhatla S, Cai SX (2004) J Med Chem 47:6299–6310
8. Zhang H-Z, Kasibhatla S, Kuemmerle J, Kemnitzer W, Ollis-Mason K, Qiu L, Crogan-Grundy C, Tseng B, Drewe J, Cai SX (2005) J Med Chem 48:5215–5223
9. Andreani LL, Lapi E (1960) Boll Chim Farm 99:583–587
10. Bonsignore L, Loy G, Secci D, Calignano A (1993) Eur J Med Chem 28:517–519
11. Kojima K, Ohno T, Inoue M, Mizukami H, Nagatsu A (2008) Chem Pharm Bull 56(2):173–175
12. Armetso D, Horspool WM, Martin N, Ramos A, Seaone C (1989) J Org Chem 54:3069–3072
13. Hatakeyama S, Ochi N, Numata H, Takano S (1988) J Chem Soc Chem Commun 17:1202–1204
14. Gonzalez R, Martin N, Seoane C, Marco JL, Albert A, Cano FH (1992) Tetrahedron Lett 33:3809–3812
15. Madhushaw RJ, Li CL, Shen KH, Hu CC, Liu RS (2001) J Am Chem Soc 123(30):7427–7428
16. Shen KH, Lush SF, Chen TL, Liu RS (2001) J Org Chem 66:8106–8111
17. Snider BB, Roush DM, Killinger TA (1979) J Am Chem Soc 101:6023–6027
18. Fuhrer C, Messer R, Häner R (2004) Tetrahedron Lett 45:4297–4300
19. Takano S, Satoh S, Ogasawara K, Aoe K (1990) Heterocycles 30:583–605
20. Ziegler E, Eder M, Belegratis C, Prewedourakis E (1967) Monatsh Chem 98:2249–2251
21. Yıldırım İ, Koca İ (2005) Kuwait J Sci Eng 32(1):49–60
22. Yıldırım İ, Koca İ, Dinçer M (2008) J Chem Soc Pak 30(1):134–141
23. Lee C, Yang W, Parr RG (1988) Phys Rev B 37:785–789
24. Becke AD (1993) J Chem Phys 98:5648–5652
25. Ditchfield R, Hehre WJ, Pople JA (1971) J Chem Phys 54:724–728
26. Frisch MJ, Trucks GW, Schlegel HB, Scuseria GE, Robb MA, Cheeseman JR, Montgomery JA Jr, Vreven T, Kudin KN, Burant JC, Millam JM, Iyengar SS, Tomasi J, Barone V, Mennucci B, Cossi M, Scalmani G, Rega N, Petersson GA, Nakatsuji H, Hada M, Ehara M, Toyota K, Fukuda R, Hasegawa J, Ishida M, Nakajima T, Honda Y, Kitao O, Nakai H, Klene M, Li X, Knox JE, Hratchian HP, Cross JB, Bakken V, Adamo C, Jaramillo J, Gomperts R, Stratmann RE, Yazyev O, Austin AJ, Cammi R, Pomelli C, Ochterski JW, Ayala PY, Morokuma K, Voth GA, Salvador P, Dannenberg JJ, Zakrzewski VG, Dapprich S, Daniels AD, Strain MC, Farkas O, Malick DK, Rabuck AD, Raghavachari K, Foresman JB, Ortiz JV, Cui Q, Baboul AG, Clifford S, Cioslowski J, Stefanov BB, Liu G, Liashenko A, Piskorz P, Komaromi I, Martin RL, Fox DJ, Keith T, Al-Laham MA, Peng CY, Nanayakkara A, Challacombe M, Gill PMW, Johnson B, Chen W, Wong MW, Gonzalez C, Pople JA (2004) Gaussian 03. Revision E.01. Gaussian Inc., Wallingford CT
27. Foresman JB, Frisch A (1996) Exploring chemistry with electronic structure methods, 2nd edn. Gaussian Inc, Pittsburgh
28. Dennington R II, Keith T, Millam J (2007) GaussView, Version 4.1.2. Semichem Inc, Shawnee Mission, KS
29. Farrugia LJ (1997) J Appl Crystallogr 30:565
30. Bucourt R (1974) In: Eliel EL, Allinger N (eds) Topics in Stereochemistry, vol 8. John Wiley, New York, pp 159–224
31. Bruno G, Nicoló F, Rotondo A, Foti F, Risitano F, Grassi G, Bilardo C (2001) Acta Cryst C57:493–494
32. Bernstein J, Davis RE, Shimoni L, Chang N-L (1995) Angew Chem Int Ed Engl 34:1555–1573
33. Allen FH (2002) Acta Cryst B58:380–388
34. Bruno IJ, Cole JC, Edgington PR, Kessler M, Macrae CF, McCabe P, Pearson J, Taylor R (2002) Acta Cryst B58:389–397